Preparation and Structure of Platinum Group Metal Colloids: Without Solvent

L. N. Lewis* and N. Lewis

General Electric Company, Corporate Research and Development, P.O. Box 8, Schenectady, New York 12301

Received August 9, 1988

The preparation and structure of platinum group metal colloids are described. These materials are prepared by the direct reaction of the metal halide salts with SiH reducing agents such as $(EtO)_3SiH$ and $Me_2(EtO)SiH$. The structure of these and previously reported colloidal preparations are analyzed by AEM, HREM, ESCA, and XANES. These analyses show that stable, highly reduced metal colloids are produced without solvent; the colloids are stabilized by the liquid reaction products of reduction. The Pt, Rh, and Pd materials are crystalline.

Introduction

Research in metal colloids has been ongoing for over a century.[1] Convergent interest in colloids has recently come from the area of catalysis. On one hand, many groups have sought to deposit ever smaller particle size clusters onto oxide supports for applications such as autocatalytic converters, petroleum cracking, etc.[2] On the other hand, colloids have been implicated as the "real" catalytic species in ostensibly homogeneous metal-catalyzed reactions.[3]

Recent[4] work has focused on preparation of metal colloids in nonaqueous solvents, potentially more useful media for carrying out organic reactions than water. In traditional approaches to this problem, workers have made stable metal colloids in alcohol by adding soluble polymer stabilizers such as polyvinyl alcohols.[5] Several groups have employed metal atom generators to prepare stable metal colloids in low dielectric constant solvents such as acetone and toluene.[6]

Work in our laboratories has been inspired by the discovery that platinum colloids are a key catalytic species in the "homogeneous" platinum-catalyzed hydrosilylation reaction.[3a] We reported the preparation and catalytic activity of platinum metal colloids in benzene and methylene chloride. These colloids were prepared by SiH reduction of some platinum metal complexes. We now wish to report a method for preparation of a new class of platinum group metal colloids and their structure as determined by analytical electron microscopy (AEM) and high-resolution electron microscopy (HREM). These colloids are prepared by direct addition of metal salts to SiH containing reducing agents.[7] The catalytic activity of these colloids in the hydrosilylation reaction will be discussed in a following report.[8]

Experimental Section

General Methods. Most operations were carried out in air under ambient conditions unless otherwise specified. NMR spectra were recorded, by using either a Varian EM 390 NMR spectrometer (^1H, 90 MHz) or a Varian XL 300 NMR spectrometer (^{13}C, 75.43 MHz; ^{29}Si, 59.3 MHz; ^{195}Pt, 64.12 MHz; Na_2PtCl_6 at 0 ppm, external standard). ESCA measurements were made by using a Surface Science Laboratories SSX-100 small-spot ESCA, the carbon is binding energy for 284.6 eV was used as an internal standard. The AEM analyses were performed on a Hitachi H-600-1 operated at 100 kV and equipped with an EEG Ortec Si(Li) energy-dispersive X-ray detector. Elemental analyses for elements having an atomic number greater than Na were obtained from X-rays generated with a focused electron probe approximately 10 nm in diameter. The HREM was performed on a Philips EM 430 instrument operated at 300 kV. Metal analyses on the colloid solutions were carried out by weighing and evaporating the solutions in Teflon beakers, dissolving with HF, HNO_3, and HCl, and then heating to drive off the Si compounds. The metal analyses were performed by ICP emission spectroscopy using an Instrumentation Laboratory Plasma 200 instrument. The XANES measurements were made at the Brookhaven National Laboratory National Light Source, zero energy was taken at the L_{III} edge of platinum metal (using Pt foil) at 11 568.4 eV with electron energy of 2.5 GeV. Data were collected in the fluorescence mode, and normalized plots of the near-edge (Figures 7 and 8 and Figures S-4,5 and 6, supplementary material (see paragraph at the end of the paper)) were produced by using published procedures.[9]

Colloid Preparations. General. The colloids described here were prepared by slow addition of the solid metal chlorides to SiH-containing liquids. The Pt colloids were "stable" as judged by the absence of any precipitate formation after at least 1 week under ambient conditions. Filtered colloidal solutions of the other metals, prepared by addition of the metal chloride to the SiH fluid alone, did show precipitate formation after standing for a few days at room temperature. Qualitatively the stability of the colloids

(1) (a) Faraday, M. *Philos. Trans.* **1857**, *147*, 145. (b) Paal, C.; Amberger, C. *Chem. Ber.* **1904**, *37*, 124. (c) Skita, A.; Meyer, W. A. *Chem. Ber.* **1912**, *45*, 3579.

(2) Bradley, J. S.; Hill, E.; Leonowicz, M. E.; Witzke, H. *J. Mol. Catal.* **1987**, *41*, 59, and references therein.

(3) In addition to our work on hydrosilylation ((a) Lewis, L. N.; Lewis, N. *J. Am. Chem. Soc.* **1986**, *108*, 7228) and hydrogenation ((b) Lewis, L. N. *J. Am. Chem. Soc.* **1986**, *108*, 743), several groups have identified or implied that colloidal species are the actual catalytic species in "homogeneous" catalyst systems. (c) Picard, J. P.; Dunogues, J.; Elyusufi, A. *Synth. Commun.* **1984**, *14*, 95. (d) Freeman, F.; Kappos, J. C. *J. Am. Chem. Soc.* **1985**, *107*, 6628. (e) Maier, W. F.; Chettle, S. J.; Rai, R. S.; Thomas, G. *J. Am. Chem. Soc.* **1986**, *108*, 2608. (f) Burk, P. L.; Pruett, R. L.; Campo, K. S. *J. Mol. Catal.* **1985**, *33*, 1.

(4) Hatschek, E.; Thorne, P. C. L. *Proc. R. Soc. London, A* **1923**, *103*, 276.

(5) (a) Nakao, Y.; Kaeriyama, K. *Bull. Chem. Soc. Jpn.* **1987**, *60*, 4465. (b) Hirai, H.; Ohtaki, M.; Komiyama, M. *Chem. Lett.* **1986**, 269. (c) Stenius, P. World Patent, International Publication Number WO 81/02688, 1981. (d) Fendler, J.; Kurihara, K. In *Metal-Containing Polymeric Systems*; Sheats, J. E., Carraher, C. E., Pittman, C. U., Eds.; Plenum: New York, 1985; p 341. (e) Koelmans, H.; Overbeek, J. Th. G. *Discuss. Faraday Soc.* **1954**, *18*, 52. (f) Rampino, L. D.; Nord, F. F. *J. Am. Chem. Soc.* **1941**, *63*, 2745.

(6) (a) Franklin, T.; Klabunde, K. J. *ACS Chem. Ser.*, in press. (b) Cardenas-Trivino, G.; Klabunde, K. J.; Dale, E. B. *Langmuir* **1987**, *3*, 986. (c) Klabunde, K. J.; Imizu, Y. *J. Am. Chem. Soc.* **1984**, *106*, 2721. (d) Lin, S.-T.; Franklin, M. T.; Klabunde, K. J. *Langmuir* **1986**, *2*, 259. (e) Klabunde, K. J.; Tanaka, Y. *J. Mol. Catal.* **1983**, *21*, 57. (f) Andrews, M. P.; Ozin, G. A. *J. Phys. Chem.* **1986**, *90*, 2929. (g) Ozin, G. A. *CHEMTECH* **1985**, 488. (h) Spalding, B. J. *Chem. Week* **1986**, *July 16*, 35. (i) Kimura, K.; Bandow, S. *Bull. Chem. Soc. Jpn.* **1983**, *56*, 3578.

(7) At least two reports discuss this type of reaction. However in neither case were colloids implicated as the products. (a) Fish, J. G. U.S. Patent 3 576 027, 1971. (b) Chalk, A. J.; Harrod, J. F. U.S. Patent 3 296 291, 1967.

(8) Lewis, L. N., manuscript in preparation.

(9) Wong, J.; Lytle, F. W.; Messmer, R. P.; Maylotte, D. H. *Phys. Rev. B* **1984**, *30*, 5587.

0897-4756/89/2801-0106$01.50/0

Table I. Preparation and Analysis of Colloids

metal salt	amt, g (mmol) (as metal)	amt of $Me_2(EtO)SiH$		amt of D_4^{vi}		metal, %	
		g	mmol	g	mmol	theor	found
$PtCl_4$	0.06 (0.3)	3.8	0.036	0	0	1.5	1.0
$RhCl_3$	0.04 (0.39)	3.9	0.038	0	0	1.0	0.2
$RhCl_3$	0.04 (0.39)	3.9	0.038	1.2	0.013	0.8	0.8
$RuCl_3$	0.043 (0.42)	4.2	0.041	1.7	0.02	0.7	0.39
$IrCl_3$	0.053 (0.28)	5.5	0.052	2.2	0.026	0.69	0.07
$OsCl_3$	0.058 (0.3)	5.5	0.052	2.2	0.026	0.74	0.13

was Pt > Rh > Ru ~ Os ≫ Pd. The Rh, Ru, and Os colloids were stable in the presence of the vinyl silicone stabilizer, whereas the Pd colloid was never stable more than 1 day.

Pt. In a typical experiment, $PtCl_4$ (0.1 g, 0.3 mmol) was slowly added to $Me_2(EtO)SiH$ (5 mL, 18.2 mmol). The order of addition for the Pt and all the other metal colloid preparations was critical. Note that the metal salt is added to the silane. After a brief induction period, gas evolution is noted and the colorless solution takes on a yellow and finally dark orange color. **Caution**: a few of these preparations have spontaneously ignited due to the presence of hydrogen and finely divided metal. ^1H NMR (C_6D_6) of initial $Me_2(EtO)SiH$: δ 4.53 (q, SiH), 3.63 (q, CH_2), 1.10 (t, CH_3 of EtO), 0.9 (d, CH_3). After addition of $PtCl_4$: loss of SiH and δ 0.9 resonance, new overlapping ethoxide resonances grow in, new resonances at δ 0.32 and 0.03, both singlets. ^{29}Si NMR (acetone and C_6D_6, with and without $Cr(acac)_3$), $Me_2(EtO)SiH$ δ +3.16. Spectrum run 12 h after reaction, chemical shift (rel integrated intensity, SiH/no SiH by gated decoupling): δ +3.16 (1, SiH), −5.59 (0.38, no SiH), −6.78 (0.09, SiH), −11.97 (0.1, no SiH), −13.79 (0.12, no SiH); after 3 days: δ +3.16 (consumed), −5.69 (0.35, no SiH), −7.49 (0.13, no SiH), −13.79 (0.11, no SiH), −22 (1, D_4 (D_4 = octamethylcyclotetrasiloxane)). Field desorption mass spectroscopy (FDMS) analysis showed peaks at 264, 280, and 296 amu, consistent with the last three species of Scheme I.

Preparation and Analysis. Table I shows the amounts of reagents used to prepare the Pt and Rh colloids directly with $Me_2(EtO)SiH$ and the Rh, Ru, Ir, and Os colloids with $Me_2(EtO)SiH/0.5D_4^{vi}$ (D_4^{vi} = tetramethyltetravinylcyclotetrasiloxane). In all cases reactions were carried out until H_2 evolution ceased and then the solutions were filtered through 0.5-μm Millipore filters. The Pd colloid was made in an analogous way by using 0.1 g of $PdCl_2$, 3.79 g of $Me_2(EtO)SiH$, and excess D_4^{vi} (4.6 g); Pd analysis, after filtration, showed 0.03% Pd.

H_2 Evolution. $PtCl_4$ (0.05 g, 0.15 mmol) was slowly added to $Me_2(EtO)SiH$ (18.2 mmol). A total of 25.5 mL (1 mmol) of H_2 was evolved as measure by a gas buret. This amount of hydrogen represents 11% of the total calculated on the basis of total SiH/2. Addition of more $PtCl_4$ resulted in further gas evolution; seven aliquots were required to complete gas evolution from this experiment. Analysis of the solution after the addition of the seventh aliquot of $PtCl_4$ by GCMS showed that a mixture was present that contained the following: $[(EtO)(Me)_2Si]_2$, *m/e* 207 (M^+ + 1), 177 (M − Et), 149 ($(EtO)_2SiMe_2$ + 1), 133 ($(EtO)_2SiMe$); $[(EtO)Me_2SiOSiMe_2Cl]$, *m/e* 197 (M^+, ^{35}Cl), 169, 133; $[Me_2(EtO)Si]_2$ − O, *m/e* 207 (M^+ + 1), 177, 163, 151, 135; D_4, *m/e* 281 (M^+ − Me).

Karstedt's Catalyst Structure: ***NMR Spectra for***

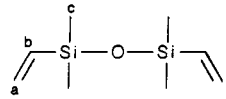

^1H NMR (C_6D_6) δ 5.88 (m, a, b), 0.17 (s, c), ($CDCl_3$) 5.83 (m, a, b), 0.07 (s, c). ^{13}C NMR (C_6D_6) δ 139.67 (b), 131.78 (a), 0.53 (c), (CD_2Cl_2) 139.88 (b), 131.77 (a), 0.48 (c). ^{29}Si NMR (C_6D_6) δ −3.02.

NMR Spectra for Karstedt's Catalyst Solution:

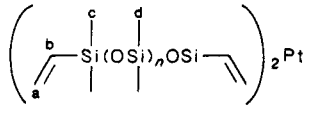

^1H NMR (xylene-vacuum transferred, replaced by C_6D_6) δ 3.37 (m, a, b), 0.47, 0.27, 0.12, −0.2, −0.3 (all singlets, c, d). ^{13}C NMR (C_6D_6) δ 56.40 ($J(^{13}C-^{195}Pt)$ = 61.5 Hz, a), 56.64 ($J(^{13}C-^{195}Pt)$ = 56.6 Hz, b), 57.19 ($J(^{13}C-^{195}Pt)$ = 60.2 Hz, a), 57.84 ($J(^{13}C-^{195}Pt$ = 61.7 Hz, b), 1.99, 1.78, 1.68, 1.44, 0.57, −1.86, −2.04 (all singlets, c, d). ^{29}Si NMR (C_6D_6) δ 8.77, 4.08, 3.86, 3.69, 3.03, 2.74 (minor peaks, c), −2.93, −3.85 (major peaks, c), −19.83, −20.62, −20.86 (major peaks, d). FDMS: M^+_n = structure I; *n* = 0, 186 amu.

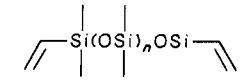

I

Found *m/e* $(186)_n$, *n* = 0–9, major peaks at 1116, 1302, and 1488.

Colloid 2. First an authentic sample of $[(EtO)_3SiC_2H_4SiMe_2]_2O$ was prepared by reacting divinyltetramethyldisiloxane (1 mL, 4.35 mmol) with $(EtO)_3SiH$ (1.63 mL, 9.7 mmol) neat and heating to 120 °C for 1 min in the presence of 5 μL of 5% Pt Karstedt's catalyst solution. Analysis by GC showed complete addition of 2 equiv of $(EtO)_3SiH$ had occurred. ^1H NMR analysis showed a mixture of B,B′ (75%) and B,A (25%) was present, δ 3.82 (overlapping q, 7 Hz), 1.18 (overlapping t, 7 Hz), 0.73 (s), 0.28 (s), 0.09 (s). Colloid **2** was prepared by slow addition of 5-μL aliquots of $(EtO)_3SiH$ (0.027 mmol) to a C_6D_6 (0.5 mL, 0.13 mmol Pt) solution in a 5-mm NMR tube. The ^1H NMR showed that when 55 μL of $(EtO)_3SiH$ had been added the vinyl groups in Karstedt's catalyst were consumed. A black solution resulted, and the NMR spectrum exactly matched that for the 2:1 $(EtO)_3SiH$ and I described above; no ^{195}Pt NMR signals were observed for the solution after the reaction.

ESCA Analysis of $CuCl_2$/SiH Products. The green solution obtained after reaction of a methanol solution of $CuCl_2$ with $(EtO)_3SiH$ was evaporated and analyzed by ESCA. The $2p^3$ binding energies were found to be 932.4, 934.4, and 936.3 eV. These data and the 2p Auger binding energy found at 570.4 eV are consistent with Cu^I.

Results and Discussion

Synthesis and Structure of Metal Colloids. Platinum. Under the best conditions, the platinum colloids made by reduction of solutions of platinum metal complexes with SiH compounds had limited stability. For example, when a methylene chloride solution of (COD)$PtCl_2$ was reacted with excess $(EtO)_3SiH$, the resulting colloid would agglomerate after a few days storage at room temperature (eq 1).[3a]

$$\text{CODPtCl}_2 + \text{excess } (EtO)_3SiH \xrightarrow{CH_2Cl_2} [Pt^0]_x + H_2 + \text{silicon products} \quad (1)$$

colloid 1

↓ 2-3 days

macroscopic Pt particles

In contrast, the direct addition of solid $PtCl_4$ to $(EtO)_3SiH$ gave a stable platinum colloid. During the slow addition of $PtCl_4$ to $(EtO)_3SiH$ there was an induction period followed by H_2 evolution. The hydrogen appeared to evolve from the surface of the solid $PtCl_4$ particles. The rate of gas evolution increased with time, and the solution took on a yellow and then finally a dark orange color. Analysis of the resulting solution proved difficult. The trialkoxy components of the starting material and product(s) were unstable toward condensation; even brief ex-

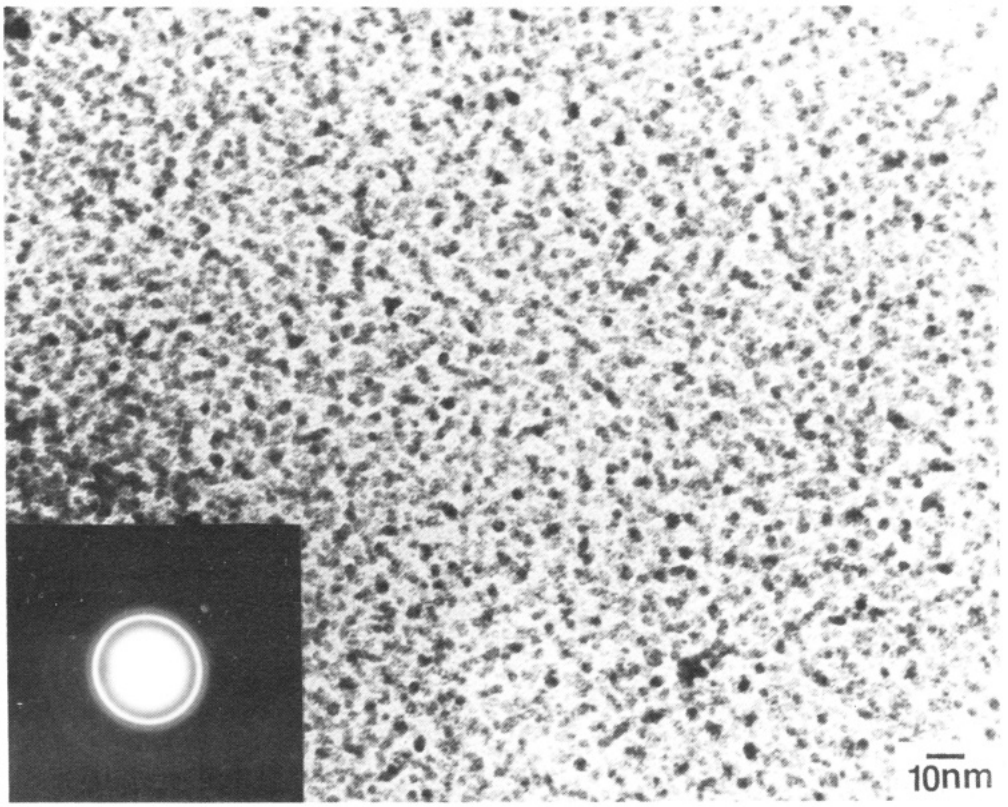

Figure 1. AEM for the Pt colloid from eq 2. Inset shows electron diffraction pattern for the Pt colloid of eq 2. Indexes to crystalline Pt.[12]

posure to moist air caused polymerization with concomitant increased viscosity and eventual formation of a solid mass. ^1H and ^{29}Si NMR showed that complicated mixtures were present, and attempts to analyze these by AEM were foiled by the cross-linking reaction.

A reducing agent that was not prone to condensation was sought. Solid $PtCl_4$ did not react with Et_3SiH at room temperature.[7b] The silane $Me_2(EtO)SiH$ proved sufficiently reactive with the metal salt to form the colloid, and cross-linking of the silane product did not occur. Thus it was possible to analyze the silicon products from the reaction (eq 2).

$$PtCl_4 + \text{excess } Me_2(EtO)SiH \rightarrow [Pt^0]_x + H_2 + \text{silicon products} \quad (2)$$

^{29}Si NMR analysis of the reaction products from eq 2 showed that the final major silicon product formed was octamethylcyclotetrasiloxane (D_4), presumably via hydrolysis of the ethoxide group. The initial product formed had a ^{29}Si NMR resonance at −5.6 ppm. Assignment of this peak is based on resonances for model compounds:[10] $[Me_3Si]_2$ has a ^{29}Si chemical shift at −20 ppm, whereas substitution of a methyl with an ethoxide causes a +14 ppm shift; thus one would calculate −6 ppm for $[Me_2(EtO)Si]_2$. On the basis of group chemical shifts, the calculated ^{29}Si NMR resonance for $[Me_2(EtO)Si]_2$ would be −0.2; with measured shifts for Me_3SiH at −16.3, $[Me_3Si]_2$ at −20 and the starting SiH, $Me_2(EtO)SiH$ at +3.48. Gated decoupling confirmed that no SiH was associated with the −5.6 resonance. Finally, ^1H NMR of the initial product solution from eq 2 showed that a new methyl resonance (singlet) formed, upfield from $Me_2(EtO)SiH$ consistent with silicon without hydrogen, containing 0 or 1 oxygen/silicon. Therefore, we conclude that the silicon product of eq 2 is the disilane, $[Me_2(EtO)Si]_2$.

Scheme I

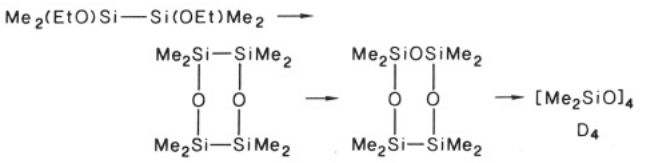

The solution from eq 2 was analyzed by ^{29}Si NMR, gas chromatography/mass spectroscopy (GCMS), and field desorption mass spectroscopy (FDMS) as it aged in air. The proposed sequence of events is summarized in Scheme I. The disilane was ultimately oxidized to siloxanes; each of the species shown in the scheme were observed by mass spectroscopy. Hydrolysis of the ethoxy group completed the sequence, which forms the D_4 final product.

In the strict absence of air there was no reaction between $PtCl_4$ and $Me_2(EtO)SiH$; however, addition of air to a mixture containing the solid platinum salt and the silane immediately caused gas evolution. This latter result was reminiscent of the fact that platinum-catalyzed hydrosilylation depends on catalytic amounts of oxygen.[11] The hydrogen evolved was measured by using a gas buret. $PtCl_4$ was added in 50-mg aliquots to 5 mL of $Me_2(EtO)SiH$ until H_2 evolution stopped. Carried out in this way, 11% of all hydrogen, based on SiH/2, was evolved. It is not known why hydrogen evolution stops.

Analytical electron microscopy (AEM) and high-resolution electron microscopy (HREM) were used to characterize the particle size and shape, elemental constituents,

(10) Williams, E. A.; Cargioli, J. D. In *Annu. Rep. NMR Spectrosc.* Webb, G. A., Ed.; Academic: London, 1979; p 221.

(11) Harrod, J. F.; Chalk, A. J. In *Organic Synthesis via Metal Carbonyls*; Wender, I., Pino, P., Eds.; Wiley: New York, 1977; Vol. 2, p 673, but especially pp 682–3: "The oxygen effect is common knowledge among people who run hydrosilylations on a large scale, where deliberate aeration of the reaction may be required to sustain catalytic activity." This effect is not understood, but we are currently investigating this very puzzling phenomenon.

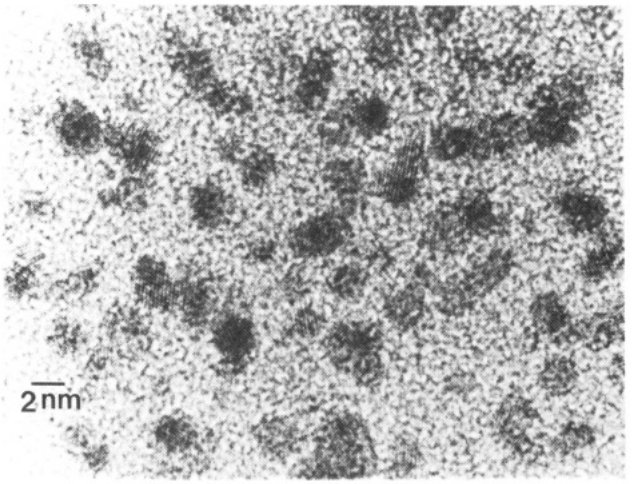

Figure 2. HREM for the Pt colloid of eq 2; 1–5-nm particles are evident. Note the diffraction fringes of the 111 planes.

and crystalline nature of the colloid particles. Figure 1 shows the small (ca. 2.5 nm) nonagglomerated particles were present in the solution from reaction 2, after evaporation on an amorphous carbon film supported by a copper grid. X-ray spectroscopy using the AEM showed that the dark spots contained Pt, Si, and O. Platinum levels were lower in the background areas, probably due to excitement of adjacent particles since the inner particle distance is on the order of the electron probe size. The electron diffraction pattern (Figure 1) for the colloid from eq 2 indexed to crystalline platinum.

The most spectacular results were obtained by HREM. As shown in Figure 2, 2-nm-diameter crystalline particles were present. The images in Figure 2 were formed by placing an aperture around the 111 diffraction ring, resulting in an interference pattern that exhibited fringes having the spacing of the 111 plane for crystalline platinum (0.2265 nm).

The technique of platinum metal salt reduction was a general one for a variety of platinum compounds and SiH reducing agents. Several salts of platinum reacted with $(EtO)_3SiH$ to give off H_2 and form the characteristic yellow Pt colloid. These salts include $PtCl_2$, PtO_2, and H_2PtCl_6. Other reducing agents employed, in addition to $Me_2(EtO)SiH$ and $(EtO)_3SiH$, include $Me(EtO)_2SiH$, Cl_3SiH, $H(Me)_2SiOSi(Me)_2H$, and $[MeSi(H)O]_4$.

Additional experiments were carried out to learn more about the nature of the platinum product from eq 2. Resonances with ^{195}Pt coupling were *not* observed in either the ^1H or ^{29}Si NMR spectra. We employed ESCA to analyze evaporated films of the colloid and compared these to model compounds (Table II). The sample, Karstedt's catalyst, is a Pt^0–tetraolefin complex, typically employed

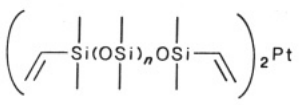

Karstedt's catalyst, $n = 0$–9

by industry as a hydrosilylation catalyst.[13] This complex was proposed to have a structure analogous to that of $(COD)_2Pt$.[14] This conclusion was confirmed by the ^{195}Pt NMR spectrum, which showed that $(COD)_2Pt$ had a resonance at −1577 ppm, while three closely spaced resonances for Karstedt's catalyst were observed at −1577.8, −1576.7, and −1577.0 ppm. The observation of three resonances for Karstedt's catalyst was attributed to the slight polymerization of the divinyltetramethyldisiloxane ligand. Note that no ^{195}Pt NMR signals have been observed for any of the colloid preparations. A colloid is expected to have a multitude of states, so that failure to observe a single ^{195}Pt resonance or any M – ^{195}Pt coupling is not surprising.[15] It would appear from the ESCA data that the platinum in the solution of reaction 2 is highly reduced. For small metal clusters, binding energy is expected to increase as the bulk metal limit is approached. A binding energy less than or equal to that for bulk metal would be expected for a colloid.[16]

Table II. ESCA Analysis of Some Pt Materials

sample	Pt $f_{7/2}$ binding energy, eV
Pt from eq 2	70.8 ± 0.4
Pt foil	71.09
Karstedt[a]	72.49
$PtCl_2$	73.46
$(COD)PtCl_2$	73.81
PtO_2	75.00

[a] Reduced platinum catalyst (Pt^0) with divinyltetramethyldisiloxane in xylene.

Rhodium. The reaction of eq 2 for Pt colloid preparation was extended to other metals. It was found that the reaction that occurred when $RhCl_3$ was slowly added to SiH compounds such as $(EtO)_3SiH$ or $Me_2(EtO)SiH$ (eq 3), was qualitatively the same as the platinum case. Slow

$$RhCl_3 + Me_2(EtO)SiH \rightarrow H_2 + [Rh^0]_x + \underset{\text{bulk metal}}{[Rh^0]_y\downarrow} + \text{soluble silicon products} \quad (3)$$

H_2 evolution occurred as the solid $RhCl_3$ was added to the silane. The rate of hydrogen evolution gradually increased as a maroon color formed in the solution. Unlike the platinum reaction of eq 2, significant formation of macroscopic size particles (Rh metal) occurred in reaction 3. Rhodium was apparently reduced to bulk metal more readily than platinum. This latter observation was demonstrated by comparing the metal analyses of the products of eq 2 and 3 after filtration through a 0.5-μm filter. The platinum solution typically contained 1.1% platinum (calcd 1.5%), whereas the rhodium solution contained 0.2% rhodium (calcd 1.0%), indicating that a large proportion of the rhodium was lost as bulk precipitate.

It was assumed that the hydrogen evolved during colloid preparation caused the bulk metal precipitation in the rhodium case. Direct reaction of either $PtCl_4$ or $RhCl_3$ with H_2 resulted in bulk precipitation of insoluble metal. The deleterious effects of H_2 during colloid synthesis could be avoided by employing a hydrogen acceptor. If exactly 0.5 mol equiv of cyclohexene per mole of SiH were added during the $RhCl_3$ reduction (eq 4), a higher yield of rhodium colloid was obtained, with bulk rhodium metal formation minimized. In this case 82% yield of soluble Rh colloid was found by analysis in solution after filtration, based on $RhCl_3$. Cyclohexene was quantitatively converted to cyclohexane in the reaction of eq 4. Settling out of the Rh colloid occurred after a few days. It was found, however, that if a vinyl silicone such as D_4^{vi} (tetramethyl-

(12) X-ray Powder Data File, ASTM Special Technical Publication, 48-J, American Society for Testing Materials, Philadelphia, PA, 1960, Card 4-0802.

(13) (a) Karstedt, B. D. U.S. Patent 3 775 452, 1973. (b) Ashby, B. A.; Modic, F. J. U.S. Patent 4 288 345, 1981.

(14) Chandra, G.; Lo, P. Y. *Organometallics* **1987**, *6*, 191.

(15) Slichter, C. P. *Surf. Sci.* **1981**, *106*, 382.

(16) For small metal clusters, binding energy is expected to increase as the bulk metal limit is approached. A binding energy less than or equal to that for bulk metal would be expected for a colloid. Morse, M. D. *Chem. Rev.* **1986**, *86*, 1049.

$$0.015RhCl_3 + Me_2(EtO)SiH + 0.5 \bigcirc\!\!\!\!\bigcirc \longrightarrow [Rh^0]_x \text{ (soluble)} + \text{silicon products} + \bigcirc \quad (4)$$

$$0.01RhCl_3 + Me_2(EtO)SiH + 0.5D_4^{vi} \longrightarrow [Rh^0]_x \text{ (soluble)} + D_4 + \text{silicon products} \quad (5)$$

tetravinylcyclotetrasiloxane) was used in place of cyclohexene as the hydrogen acceptor, no settling out of the rhodium colloid occurred after at least 1 week (eq 5).

Analysis of the silicon products from eq 3 and 5 by ^{29}Si and ^1H NMR, GCMS, and FDMS showed that the same product mixture was obtained in the rhodium reactions as in the platinum reactions. In neither the platinum nor rhodium reactions were any molecular species containing metal observed. No Si–metal coupling was observed by NMR. No metal-containing species were observed in the mass spectrum.

The platinum and rhodium colloid mixtures were analyzed by Raman spectroscopy. The high vapor pressure of $Me_2(EtO)SiH$ precluded analysis of the colloids based on this reducing agent due to heating and evaporation in the laser beam. Both platinum and rhodium colloids were prepared by addition of the metal chloride salts to $Me_2HSiOHSiMe_2$. In both cases the symmetric SiO stretch from the starting silane moved to lower energy after reaction with the metal salts (544 to 495 cm^{-1}). The reduction in energy of the SiOSi stretch may be due to the formation of new siloxane bonds and/or interaction of the siloxane with the metal. For the Pt case a new peak was observed at 120 cm^{-1}, whereas in the Rh case a new peak was observed at 170 cm^{-1}. These latter peaks may be due to the metal–metal stretch in the colloids.

AEM (Figure S-1, supplementary material) and HREM (Figure 3) were used to analyze the rhodium colloids from eq 3. In a fashion analogous to that for platinum, the rhodium colloids displayed interference fringes from the 111 planes of the 2-nm-diameter rhodium crystallites. The rhodium particles appear to have a greater tendency to agglomerate than the platinum particles did. The diffraction pattern for the rhodium colloid indexed to crystalline rhodium. X-ray spectroscopy showed rhodium, silicon, and oxygen. The rhodium concentration was higher in the area of the dark spots than in the background region.

The rhodium products from the reaction in eq 3 were analyzed by ESCA and compared to model rhodium compounds. As shown in Table III, the rhodium colloid was analyzed in two ways. In the "air" case the product solution was simply evaporated in air on a Teflon sample stub and then in the vacuum chamber of the ESCA instrument. In the "inert" sample, the colloid was prepared in a nitrogen-filled glovebox, evaporated in the glovebox on the sample stub, and then transferred without air exposure to the instrument vacuum chamber. The platinum colloid showed an ESCA signal with a low binding energy after preparation in air. However, there was a significant difference between the binding energy for the rhodium colloid prepared in the glovebox and that prepared in air. This result was consistent with surface oxidation of the rhodium colloid. The value for the binding energy of the rhodium colloid (inert) closely matched that for $Rh_6(CO)_{16}$. Note

(17) Wagner, C. D.; Gale, L. H.; Raymond, P. *Anal. Chem.* **1979**, *51*, 466.

Table III. ESCA Data for Rhodium Materials

sample	Rh $3d_{5/2}$ binding energy, eV
Rh foil (this work)	306.9
Rh foil (ref 17)	307.2
$Rh_6(CO)_{16}$ (ref 17)	308.6
Rh from eq 3, air	309.7
Rh from eq 3 inert	308.3
$[(COD)RhCl]_2$	308.6
$RhCl_3$	309.1

the close correspondence for the binding energy we obtained for Rh foil and the literature value. The ESCA data confirmed that the rhodium product from eq 3 was reduced relative to $RhCl_3$.

Palladium. Preparation of a stable palladium colloid was more difficult than the corresponding platinum and rhodium colloids. Addition of $PdCl_2$ to any SiH compound resulted in brief formation of a brown color in solution, immediate H_2 evolution, and deposition of macroscopic palladium particles. Analysis of the filtered solutions typically showed <0.01% Pd to be present. Stable, yellow brown, colloidal solutions of palladium were obtained by using D_4^{vi} as a hydrogen acceptor, albeit with low Pd concentrations (0.03% Pd, eq 6).

$$0.01PdCl_2 + Me_2(EtO)SiH + 0.5D_4^{vi} \longrightarrow [Pd^0]_x \text{ (colloid)} + Pd\downarrow + \text{Si products} \quad (6)$$

Analysis of the filtered solution by AEM confirmed the presence of 2.5-nm colloidal particles, Figure 4. Several of the particles shown in Figure 4 were arranged in a curious ring pattern. These rings may be intermediate structures on the way to agglomeration. The diffraction pattern for the Pd sample indexed to crystalline palladium. X-ray spectroscopy performed on the particle-free regions showed only silicon and oxygen present, whereas the dark spots showed palladium, silicon, and oxygen.

Ir, Os, and Ru. The reaction between metal salts and $Me_2(EtO)SiH$ in the presence of D_4^{vi} was extended to the other three members of the platinum group, namely, Ru, Os, and Ir. In all three cases, H_2 evolution occurred upon addition of the metal salt to the SiH/vinyl mixture. Dark, homogeneous solutions were obtained for each metal after filtration. Amorphous diffraction patterns were obtained for these three metals.

There was no reaction between $IrCl_3$ and $(EtO)_3SiH$, but H_2 evolution did occur when $IrCl_3$ was added to excess $Me_2(EtO)SiH$ and 0.5 equiv (relative to SiH) of D_4^{vi}. After filtration, a lemon–yellow solution was obtained which analyzed for 0.07% Ir. No peak assignable to an iridium-containing species was detected by FDMS analysis of the reaction solution, nor was any Si–Ir coupling observed by ^{29}Si NMR. The FDMS and ^{29}Si NMR analyses did show species such as those of Scheme I. No particles of Ir could be found by AEM analysis of the iridium reaction solution.

There was an immediate reaction between $OsCl_3$ and $(EtO)_3SiH$ to give a brown precipitate with H_2 evolution. The reaction of $OsCl_3$ proceeded in a manner analogous to that of eq 5 and 6, to give a brown solution after filtration from a brown solid. Analysis by HREM (Figure S-2, supplementary material) showed that ca. 1-nm amorphous particles were present.

$RuCl_3$ reacted with $Me_2(EtO)SiH$ and 0.5 D_4^{vi} (as in eq 5 and 6) with H_2 evolution and formation of a dichroic green (transmitted light)/brown (reflected light) solution. AEM analysis, Figure 5, showed the presence of "wormlike" structures that analyzed for ruthenium, silicon, and oxygen by X-ray spectroscopy. Analysis of the ruthenium colloid by HREM (Figure S-3, supplementary material) showed

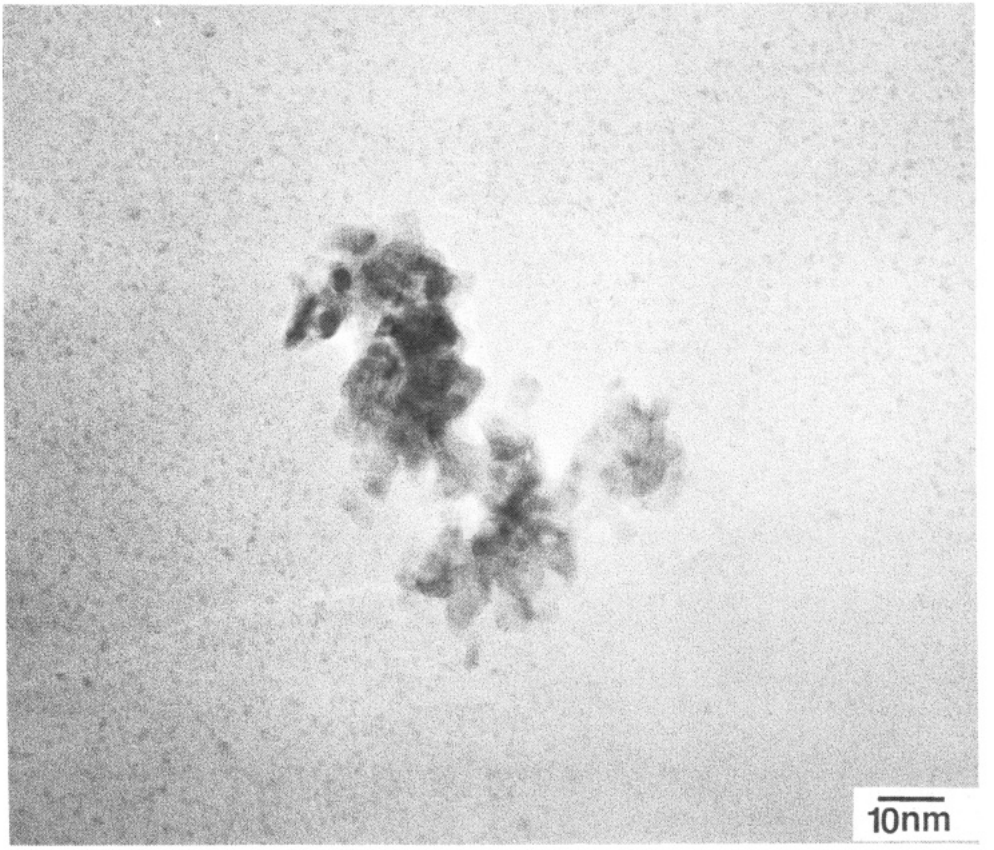

Figure 3. HREM for the Rh colloid from eq 3. Note the 111 diffraction fringes and the fact that, unlike the Pt colloid, significant particle–particle interaction occurs for Rh.

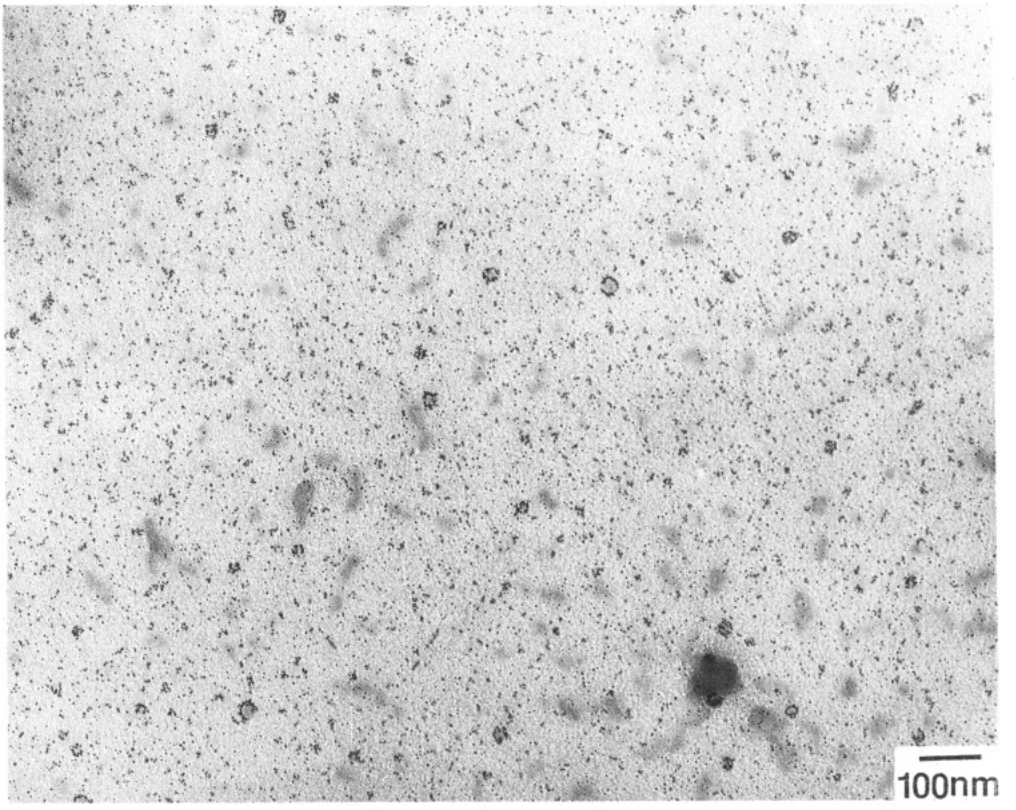

Figure 4. AEM for the Pd colloid of eq 6. Note the curious ring arrangement of the Pd particles.

the presence of 2–3-nm, partially agglomerated particles. No Ru-containing species were observed by FDMS.

An unusual observation was made while carrying out the AEM analysis of the ruthenium colloid. It was possible to "write" on the film with the electron beam. As shown in Figure 6, the electron beam was used to write the authors' name. In addition, as shown in the inset to Figure 6, the raster of the electron beam exposed lines in the film. Work is under way to determine the applicability of this material as an electron beam photoresist.

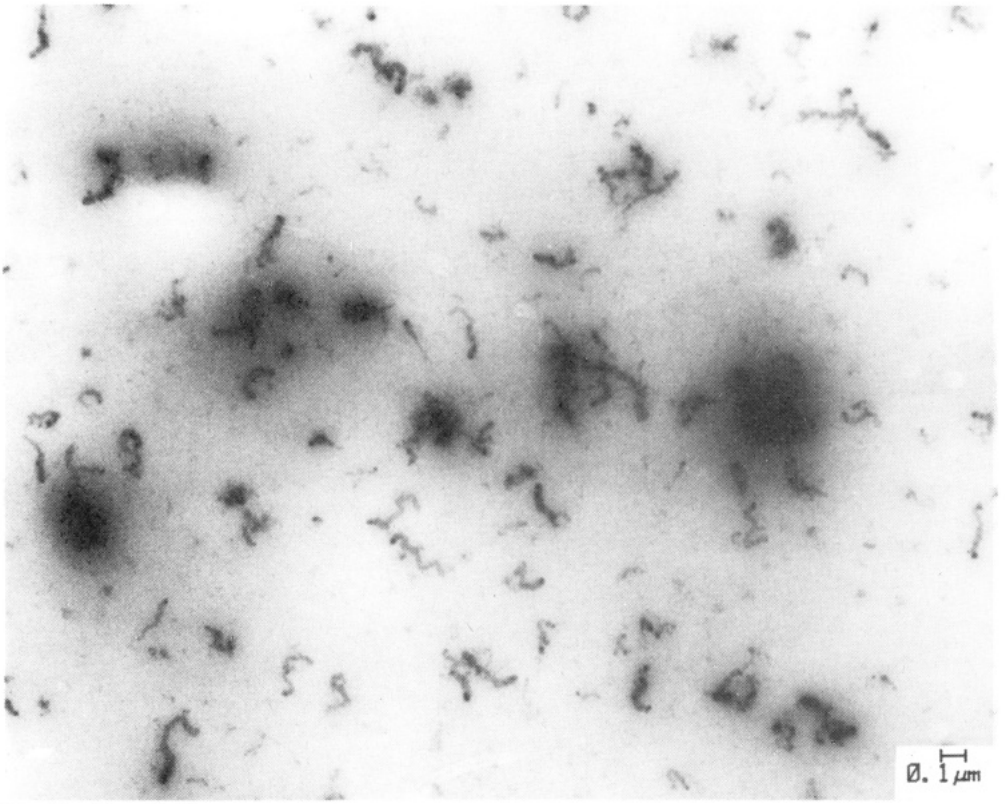

Figure 5. AEM for the Ru colloid.

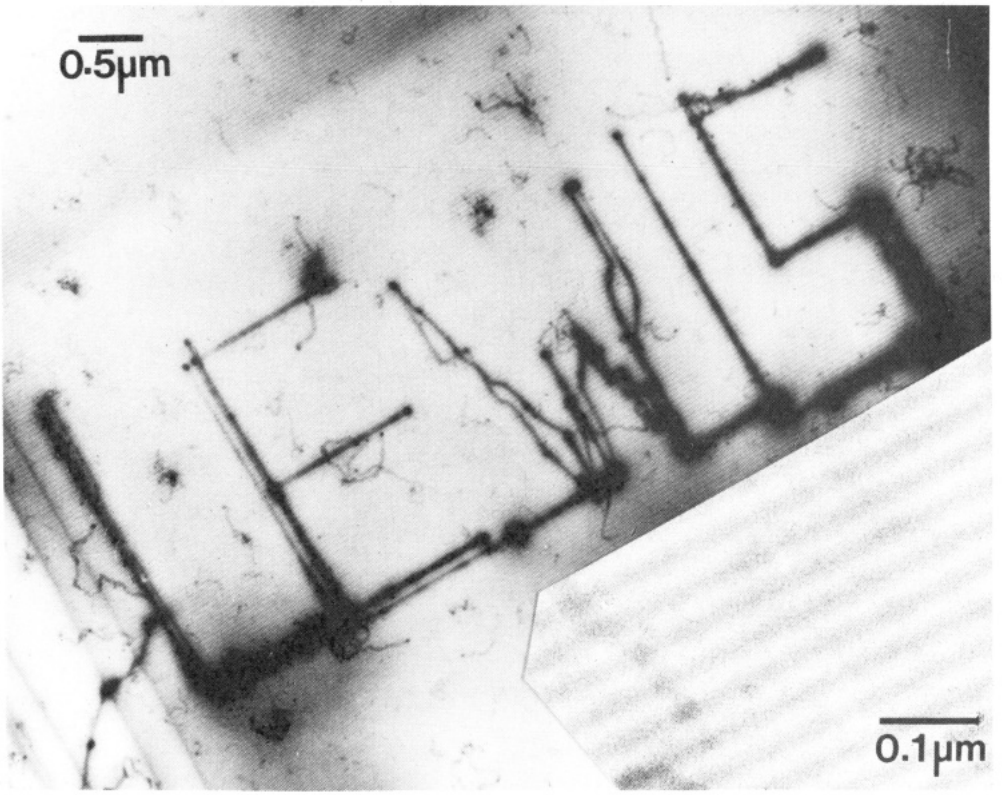

Figure 6. Ru colloid where we "wrote" on the sample with the electron beam. Inset shows Ru colloid at higher magnification. Note lines and spaces from the electron beam raster.

Beyond the Pt Group. The reaction of SiH and metal salts was extended beyond the platinum group. Standard reduction potentials for the metals suggest that the Pt group should indeed be reduced to metal^0. For nickel, cobalt, and copper, only copper is expected to be reduced to metal by SiH (the reducing power of SiH is assumed to be about equal to that of dihydrogen). In fact there was no reaction between $NiCl_2$, $CoCl_2$, or $CuCl_2$ with either $(EtO)_3SiH$ or $Me_2(EtO)SiH$. There was a reaction between $(EtO)_3SiH$ with a methanol solution of $CuCl_2$; no reaction between methanol solutions of the nickel or cobalt salts was observed. When $CuCl_2$ in methanol was slowly added to (EtO)SiH, H_2 evolved slowly with precipitation of a white solid (CuCl). The white solid redissolved, and then

the color of the solution changed to orange and then to yellow. If the solution was exposed to air, the final color was green. Analysis of the green solution by ESCA confirmed that Cu^I was the predominant species present. An electron diffraction pattern observed for the sample most closely matched that for CuCl.

A precipitate formed immediately upon addition of $HAuCl_4$ to $(EtO)_3SiH$. However, if $HAuCl_4$ was slowly added to excess $(EtO)_3SiH/0.5D_4^{vi}$, a purple solution was obtained with limited stability. The purple color is reminiscent of the well-known gold colloids.[18] After 24 h, precipitation occurred in the purple–gold solution with complete loss of color.

Colloid Structure. The actual structure of the various metal reduction products described above is not known. Colloids derive their existence from the fact that particle–particle contact is inhibited. Agglomeration is prevented by either electronic repulsion or by surface complexation of protecting groups.[2,18] It seems likely that the colloids described here obtain their stability from silicon-containing protecting groups derived from the reaction products of SiH reduction. Samples of the colloid mixtures for Pt, Rh, Ir, Os, and Ru were carefully layered onto the top of SF-96 oil (50-cSt viscosity silicone fluid). The tubes were then subjected to ultracentrifugation at 20 °C and 40 000 rpm for 24 h. With the exception of the ruthenium sample, all of the metal solutions remained intact. There was some decomposition of the ruthenium which caused dark, solid particles to precipitate to the bottom of the tube. In addition, freezing of the platinum colloidal mixture to liquid-nitrogen temperatures, followed by rewarming to ambient temperature, did not cause agglomeration. This latter result is in contrast to aqueous colloidal silica mixtures, which undergo irreversible agglomeration upon freezing.

The Pt, Rh, and Pd colloids described above are all monodisperse, average size ca. 2 nm. A 2-nm diameter particle for a fcc metal may represent an energy minimum.[19] In a fascinating report, several Russian workers describe their analysis of a "giant palladium cluster".[20] By EXAFS and HREM these workers described a 2.6-nm-diameter Pd cluster that they estimate contains 570 ± 30 Pd atoms. One can construct polyhedra composed of n monoatomic metal layers, packed around a single metal atom, in which each layer consists of $10n^2 + 2$ metal atoms. A 561-atom cluster corresponds to a five-layer icosahedron with 252 Pd atoms in the outer shell.

Synchrotron radiation (XANES) was used to analyze the Pt L_{III} edge from the colloid from eq 1 as well as for some relevant platinum model compounds. In general the area under the near-edge curve (white line) is related to the metal oxidation state. The electronic dipole transitions at the Pt L_{III} edge are from $2p^{3/2}$ core level to the empty 5d state ($\Delta J = 0 \pm 1$) and therefore the peak intensity or "white line" is proportional to the d-electron vacancies.[21] For related systems of the same metal atom, a lower white-line area is consistent with a lower metal oxidation state. The shape of the near edge is also affected by the geometry and the nature and number of ligands around the metal. Figure 7 shows the near edge spectra for (COD)$PtCl_2$ and colloid 1, its reaction product with $(EtO)_3SiH$. A similar sequence was found for Karstedt's catalyst and its reaction prooduct with $(EtO)_3SiH$, colloid 2 (Figure S-4, supplementary material). The near-edge spectra for colloids 1 and 2 were similar at the absorption edge, suggesting that they had similar electronic properties (Figure S-5, supplementary material). However, the fact that they had different fine-structure shape past the edge suggests that the Pt atoms were in slightly different environments in these colloids.

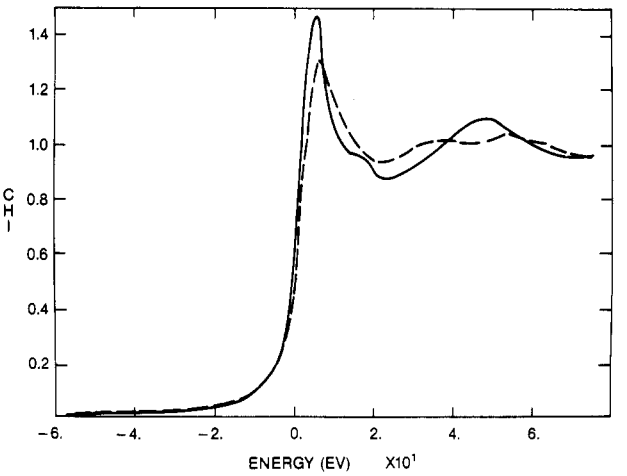

Figure 7. Near-edge spectra for (COD)$PtCl_2$ (solid line) and colloid 1, eq 1 (dashed line). Note the lower white-line intensity (area under near edge curve) for colloid 1 vs (COD)$PtCl_2$. Also note the different fine structure pattern after the near edge for the two materials, indicating that they have a different structure.

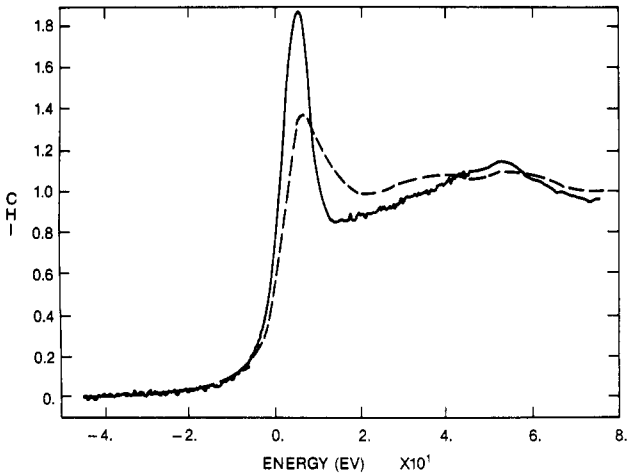

Figure 8. Comparison of the near edge for Pt aqueous colloid (solid line) and colloid 1 (dashed line). Note the difference in white-line intensity for the two colloids, which demonstrates that colloid 1 is more reduced than the aqueous Pt colloid.

Addition of a solution of colloid 2 to a vinyl-containing silicone fluid resulted in a change in its absorption edge spectrum such that it now identically matched that for Karstedt's catalyst again (Figure S-6, supplementary material). These results were consistent with a sequence in which addition of the SiH reducing agent to the platinum compound resulted in formation of a platinum colloid devoid of the vinyl silicone. Addition of the vinyl silicone recreated the environment found in Karstedt's catalyst. Finally, it was interesting to compare colloid 2 to a traditional aqueous platinum colloid, prepared by reduction

(18) Weiser, H. B. In *Inorganic Colloid Chemistry*; Wiley: New York, 1933; Vol. 1.

(19) See, for example: Sermon, P. A.; Thomas, J. M.; Keryou, K.; Millward, G. R. *Angew. Chem., Int. Ed. Engl.* **1987**, *26*, 918.

(20) Vargaftik, M. N.; Zagorodnikov, V. P.; Stolyarov, I. P.; Moiseev, I. I.; Vikholobov, V. A.; Kochubey, D. I.; Chuvilin, A. L.; Zaikovsky, V. I.; Zamaraev, K. I.; Timofeava, G. I. *J. Chem. Soc., Chem. Commun.* **1985**, 937.

(21) (a) Lytle, F. W.; Greegor, R. B.; Marques, E. C.; Biebesheimer, V. A.; Sandstrom, D. R.; Horsley, J. A.; Via, G. H.; Sinfelt, J. H. In *Catalyst Characterization Science*; Deviney, M. L., Gland, J. L., Eds.; ACS Symp. Ser. 288; American Chemical Society: Washington, D.C., 1985; p 280. (b) Lytle, F. W.; Via, G. H.; Sinfelt, J. H. In *Synchrotron Radiation Research*; Winick, H., Doniach, S., Eds.; Plenum: New York, 1980; p 401.

of H_2PtCl_6 by citrate in water.[22] As shown in Figure 8, the white-line intensity of the aqueous platinum colloid was significantly greater than that for colloid 2. The differences in white-line intensities and curve shapes demonstrated that colloid 2 has a different structure and was more reduced than the aqueous platinum colloid.

Analysis of the specific identity of the surface ligands of the Pt, Rh, and Pd colloids in this work awaits study by EXAFS. It is well-known for Pt and Rh that in the presence of terminal olefins, R_3SiH is cleanly added intact to the olefin in the presence of the metal. Very little olefin hydrogenation occurs in these systems, and no example of disilane addition has been reported; thus the surface of the colloid may be composed of R_3Si fragments and H. Indeed all of the X-ray spectroscopic analyses we have made of the dark spots (colloids) show metal, silicon, and oxygen; however, further work is needed to determine the exact nature of the surface species.

The structure of the Ru, Os, and Ir materials is more speculative. A number of workers have discussed the problem of the boundary between authentic large molecular clusters and colloids.[23] In one study, a cluster as small as Os_{10} has been shown to possess significant bulk metal properties.[24] The cluster containing $Au_{18}Ag_{20}$ has a diameter of 1.5 nm and likewise shows evidence of significant metal-band-like characteristics.[25] The Ru, Os, and Ir materials prepared here no doubt lie on the boundary of cluster and colloid, stabilized by silicon species.

This report describes a straightforward method for preparation of metal colloids in low dielectric constant media. Due to the high surface area the obvious use for the materials is in the area of catalysis.[8] As shown by the TEM/HREM analyses, it is possible to deposit the metal crystallites intact; thus these colloidal mixtures may have application for deposition of metals onto a variety of substrates.

Acknowledgment. Dr. Ernie Hall carried out the HREM measurements, Dr. Mike Burell and Mr. John Chera performed the ESCA analyses, Dr. Elizabeth Williams, Paul Donahue, and Joanne Smith carried out some of the NMR measurements and participated in helpful discussions, Winnie Balz carried out the ICP metal analyses, and Dr. Pete Codella carried out the Raman measurements. Professor Robert Crabtree, Yale University, is acknowledged for providing some key references and for valuable discussions. Dr. Joe Wong, Livermore National Laboratory, assisted in the XANES measurements and analyses.

Supplementary Material Available: AEM for Rh colloid (eq 3), HREM for Os colloid, HREM for Ru colloid, XANES spectra for various Pt colloids; all photomicrographs (6 pages). Ordering information is given on any current masthead page.

(22) Bruno, G. C. *Chem. Soc., Faraday Trans.* **1956**, *52*, 1235.
(23) (a) Schmid, G. *Nachr. Chem., Tech. Lab.* **1987**, *34*, 249. (b) Friedel, J. *J. Phys. (Les Ulis, Fr.)* **1977**, *38*, Coll. C2, suppl. 7, C2-1.
(24) (a) Benfield, R. E.; Edwards, P. P.; Stacy, A. J. *Chem. Soc., Chem. Commun.* **1982**, 525. (b) Johnson, D. C.; Benfield, R. E.; Edwards, P. P.; Nelson, W. J. H.; Vargas, M. D. *Nature (London)* **1985**, *314*, 231.
(25) Teo, B. K.; Keating, K.; Kao, Y.-H. *J. Am. Chem. Soc.* **1987**, *109*, 3494.

Centrosymmetric Crystals as Host Matrices for Second-Order Optical Nonlinear Effects†

I. Weissbuch,* M. Lahav,* and L. Leiserowitz*

Department of Structural Chemistry, The Weizmann Institute of Science, Rehovot, 76100 Israel

G. R. Meredith* and H. Vanherzeele*

E. I. du Pont de Nemours and Company, Central Research and Development Department, P.O. Box 80356, Wilmington, Delaware 19880-0356

Received August 10, 1988

Reduction of crystal symmetry via preferential occlusion of guest molecules through different subsets of crystal surface sites has been used to include centrosymmetric host crystals as a matrix for providing second-order nonlinear optical effects. The method is also applicable for generating a second harmonic signal along the principal nonpolar axis of polar crystals. This approach is illustrated by several examples. These optical measurements yield information on crystal growth processes and on the alignment of guest molecules in the host crystal.

Recent studies have revealed large molecular hyperpolarizabilities β of certain organic materials, leading to anomalously large optical nonlinearities relative to those of more conventional inorganic substances.[1-3] Second-order optical effects, such as second harmonic generation (SHG), optical rectification, sum and difference frequency mixing, and parametric generation or amplification by three-photon interactions, are all governed by a third-rank tensor.[4] Thus, to be potentially useful for these effects,

† Part of this work was done during a sabbatical leave of M.L. and L.L. in the laboratory of Dr. E. Wassermann, Du Pont.

(1) Prasad, P. N.; Ulrich, D. R. *Nonlinear Optical and Electroactive Polymers*; North-Holland; New York, 1988.
(2) Chemla, D. S.; Zyss, J. *Nonlinear Optical Properties of Organic Molecules and Crystals*; Academic: New York, 1987; Vols 1 and 2.
(3) Williams, D. J. *Nonlinear Optical Properties of Organic and Polymeric Materials*; American Chemical Society: Washington, D.C., 1983.

0897-4756/89/2801-0114$01.50/0